Cell Stem Cell
Article

# KDR Identifies a Conserved Human and Murine Hepatic Progenitor and Instructs Early Liver Development

Orit Goldman,[1,10] Songyan Han,[1,10] Marion Sourrisseau,[2] Noelle Dziedzic,[1] Wissam Hamou,[1] Barbara Corneo,[5] Sunita D'Souza,[1] Thomas Sato,[6] Darrell N. Kotton,[7] Karl-Dimiter Bissig,[8] Tamara Kalir,[3] Adam Jacobs,[4] Todd Evans,[9] Matthew J. Evans,[2] and Valerie Gouon-Evans[1,*]

[1]Department of Developmental and Regenerative Biology, Black Family Stem Cell Institute
[2]Department of Microbiology
[3]Division of Gynecologic Pathology
[4]Department of Obstetrics, Gynecology, and Reproductive Science
Icahn School of Medicine at Mount Sinai, New York, NY 10029, USA
[5]Neural Stem Cell Institute, Rensselaer, NY 12144, USA
[6]Institute of Science and Technology, Ikoma, Nara 630-0101, Japan
[7]Center for Regenerative Medicine, Boston University and Boston Medical Center, Boston, MA 02118, USA
[8]Center for Cell and Gene Therapy, Stem Cells and Regenerative Medicine Center, Department of Molecular and Cellular Biology, Baylor College of Medicine, Houston, TX 77030, USA
[9]Department of Surgery, Weill Cornell Medical College, New York, NY 10065, USA
[10]These authors contributed equally to this work
*Correspondence: valerie.gouon-evans@mssm.edu
http://dx.doi.org/10.1016/j.stem.2013.04.026

## SUMMARY

**Understanding the fetal hepatic niche is essential for optimizing the generation of functional hepatocyte-like cells (hepatic cells) from human embryonic stem cells (hESCs). Here, we show that KDR (VEGFR2/FLK-1), previously assumed to be mostly restricted to mesodermal lineages, marks a hESC-derived hepatic progenitor. hESC-derived endoderm cells do not express KDR but, when cultured in media supporting hepatic differentiation, generate KDR+ hepatic progenitors and KDR− hepatic cells. KDR+ progenitors require active KDR signaling both to instruct their own differentiation into hepatic cells and to non-cell-autonomously support the functional maturation of cocultured KDR− hepatic cells. Analysis of human fetal livers suggests that similar progenitors are present in human livers. Lineage tracing in mice provides in vivo evidence of a KDR+ hepatic progenitor for fetal hepatoblasts, adult hepatocytes, and adult cholangiocytes. Altogether, our findings reveal that KDR is a conserved marker for endoderm-derived hepatic progenitors and a functional receptor instructing early liver development.**

## INTRODUCTION

Liver disease affects millions of people worldwide. Hepatocyte transplantation is considered a potential treatment for liver diseases and a bridge for patients awaiting liver transplantation, but its application has been hampered by a limited supply of hepatocytes. Human embryonic stem cells (hESCs) established from early embryos or induced pluripotent stem cells (iPSCs) derived from somatic adult cells are pluripotent and could constitute an unlimited source of hepatocytes for cell replacement therapy (Takahashi et al., 2007; Thomson et al., 1998). Even though prior studies have established protocols to efficiently generate in vitro hepatocyte–like (hepatic) cells from hESCs (Agarwal et al., 2008; Cai et al., 2007; Duan et al., 2010; Hay et al., 2008; Touboul et al., 2010) or hiPSCs (Hannan et al., 2013; Si-Tayeb et al., 2010b; Sullivan et al., 2010), hepatic cells remain mostly inefficient at repopulating diseased livers in vivo, making a readout of their functional in vivo properties challenging. Although underlying mechanisms for the poor repopulating ability of hESC-derived hepatic cells remain unknown, recent studies have exploited the well-documented ability of the hepatitis C virus (HCV) to specifically infect functional hepatocytes, and this has demonstrated the functionality of human pluripotent stem cell-derived hepatic cells (Roelandt et al., 2012; Schwartz et al., 2012; Wu et al., 2012; Yoshida et al., 2011). Thus, the translational potential of human pluripotent stem cell-derived hepatic cells is already becoming a reality through the development of model systems for studying the host-viral interaction in HCV pathogenesis. Better insight into how various components of the hepatic niche interact will therefore have a substantial clinical impact for both organ regeneration and disease-modeling applications.

Liver organogenesis involves complex cell-cell interactions occurring in early development. In the mouse, the septum transversum and cardiac mesoderm secrete bone morphogenetic proteins (BMPs) and fibroblast growth factors (FGFs) to instruct the adjacent ventral endoderm to become hepatic endoderm (Si-Tayeb et al., 2010a). Studies in *Kdr* null embryos demonstrated that endothelial cells are required for the promotion of liver morphogenesis prior to the formation of functional blood vessels

(Matsumoto et al., 2001). Our previous work in mouse ESC differentiation cocultures revealed that endothelial cells, through regulation of Wnt and Notch pathways, also function to support hepatic specification of the endoderm (Han et al., 2011). Considering the scarcity of early human fetal tissues, hESCs provide a powerful in vitro model of early human developmental processes. In this study, we find that KDR-expressing endothelial cells coemerge with hepatic cells during hepatic differentiation of hESCs. Although KDR expression was thought to be restricted to mesodermal derivatives (Ema et al., 2006; Holmes et al., 2007) as well as to a subset of ectodermal-derived neurons (Sondell and Kanje, 2001), to our surprise, we found that a distinct population of hepatic progenitor cells characterized by KDR expression arises concurrently with hepatic cells. Our data also provide evidence for the presence of KDR+ hepatic progenitors in developing mouse and human livers, supporting the concept that KDR also marks an endoderm derivative.

## RESULTS

### Concomitant Development of KDR–CD31– Hepatic Cells, KDR+CD31– Prehepatic Cells, and KDR+CD31+ Endothelial Cells in hESC-Derived Hepatic Cultures

For generation of hESC-derived hepatic cells, the endoderm program was induced upon embryoid body (EB) formation using Activin A (Figure 1A). Endoderm induction was very robust as assessed by the high percentage of cells expressing CXCR4 and cKIT (Figure 1B, up to 95% CXCR4+cKIT+ cells at day 5), two markers reflecting the development of endoderm in mouse and human ESC differentiation cultures (D'Amour et al., 2005; Gouon-Evans et al., 2006). To test whether the day 5 CXCR4+ cKIT+ endoderm-enriched cells were devoid of mesendoderm cells, whose bipotentiality could give rise to endoderm and mesoderm cells, we examined via flow cytometry in EBs expression of PDGFRα, which has been commonly used to mark mesendoderm cells emerging from mouse or human ESC cultures (Kopper and Benvenisty, 2012; Tada et al., 2005) (Figure 1B). These data revealed that at day 4 the vast majority of cells in EBs (90.9% ± 9.3%) homogenously expressed PDGFRα, whereas at day 5 (when cells were purified for CXCR4 and cKIT expression) PDGFRα was dramatically downregulated (0.38% ± 0.18%). These data demonstrate that the day 5 CXCR4+cKIT+ population that we propose is enriched for endoderm cells is staged beyond the point of mesendoderm development. A very small percentage of a potential mesodermal progenitor population expressing VEGFR2 (KDR) (up to 2%) consistently developed within the CXCR4+cKIT+ population at day 5. In an attempt to further enrich the endoderm population from potential KDR+ mesodermal progenitors, the KDR+ cells were excluded from the day 5 CXCR4+cKIT+ fraction with the use of fluorescence-activated cell sorting (FACS) (Figure 1B). When further cultured, the day 5 CXCR4+cKIT+KDR+ cells generated mostly CD31+ endothelial cells, confirming their mesodermal potential (Figure S1A available online). The day 5 CXCR4+cKIT+KDR− enriched endoderm cell population, with purity always higher than 95% (97.36% ±1.3% for n = 15 experiments), was then cultured to allow hepatic specification in the presence of a serum-free hepatic media (described in Experimental Procedures). Immunostainings for the endoderm marker FOXA2; hepatic markers alpha fetoprotein (AFP, the first marker of hepatic specification), albumin (ALB, a marker indicative of further hepatic maturation), and HNF4α; epithelial markers cytokeratin 18 (CK18, expressed in hepatocytes and progenitor cells) and cytokeratin 19 (CK19, present in progenitors and cholangiocytes); and the endothelial marker CD31 indicated a concomitant and progressive emergence of hepatic cells with endothelial cells (Figure S1B). The specification and maturation of hepatic cells, as well as the generation of endothelial cells, was confirmed by real-time quantitative PCR (qPCR), with increasing transcript levels over time for *AFP*, *ALB*, α1-antitrypsin (*AAT*), the P450 enzymes *CYP3a7* and *CYP3a4*, and also detectable transcript levels for *HNF4α* and *CD31* (Figure S1C). Decreased transcript levels for the hepatoblast marker *CK19* provided further evidence for the maturation of the hepatic cells in culture. Even though hepatic cells express many hepatic markers found in adult hepatocytes, they also express AFP, indicative of immature hepatic cells that mostly resemble immature fetal hepatoblasts rather than mature adult hepatocytes (Figures S1B and S1C). The identity of the hepatic cells was also supported by the presence of cytoplasmic glycogen (Figure S1D).

For evaluation of the contribution of the endothelial cell lineage to these hepatic cultures, flow cytometry analyses for the endothelial markers CD31 and KDR were performed at different time points (Figures 1C, 1D, and S2A). The percentage of the KDR+CD31+ endothelial cells (hereafter termed "K+C+") was the highest at day 12 (Figures 1C and S2B with 2.7% ± 2%). To confirm their endothelial identity, we purified K+C+ cells from day 9 hepatic cultures and further cultured them in hepatic media until day 17. Immunostainings in the dish indicated that all cells maintained expression of CD31 and KDR and expressed the typical cytoplasmic endothelial marker von Willebrand factor (Figure S2C). Moreover, purified K+C+ cells formed the characteristic vascular-like network developed by endothelial cells in a matrigel assay (Figure S2D).

In addition to the K+C+ endothelial population, the flow cytometry analyses revealed two major distinct populations: the KDR+CD31− cells (hereafter termed "K+C−") and the KDR−CD31− cells (hereafter termed "K−C−") (Figures 1C, 1D, S2B, and S2E). Given that the sorted endoderm was originally negative for KDR, we set out to determine the origin of the K+C− population. Interestingly, daily flow cytometry analysis combined with immunostaining in the dish from day 7 to day 11 hepatic cultures indicated a hierarchy in the emergence of the three populations and of the cells expressing AFP and HNF4α. Expression of the early marker for hepatic endoderm, HNF4α, is induced as early as day 7, similar to KDR expression (Figure 1D). KDR staining appeared to be both cytoplasmic and at the cell membrane (Figure 1D) as seen in Huvec endothelial cells (Figure S2C). However, AFP expression is initiated after the emergence of K+C− cells and is further increased as the K+C− population expands (Figure 1D). One possibility is that K+C− cells derive from the fusion of K−C− hepatic cells with K+C+ endothelial cells (although the endothelial component of the culture represented by the K+C+ cells is very small at these early time points). Two different strategies were used to rule out fusion as a mechanism by which K+C− cells are generated. The first strategy consisted of coculturing the K−C− cells with K+C+ cells purified from day 9 HES-2-derived hepatic cultures (Figures

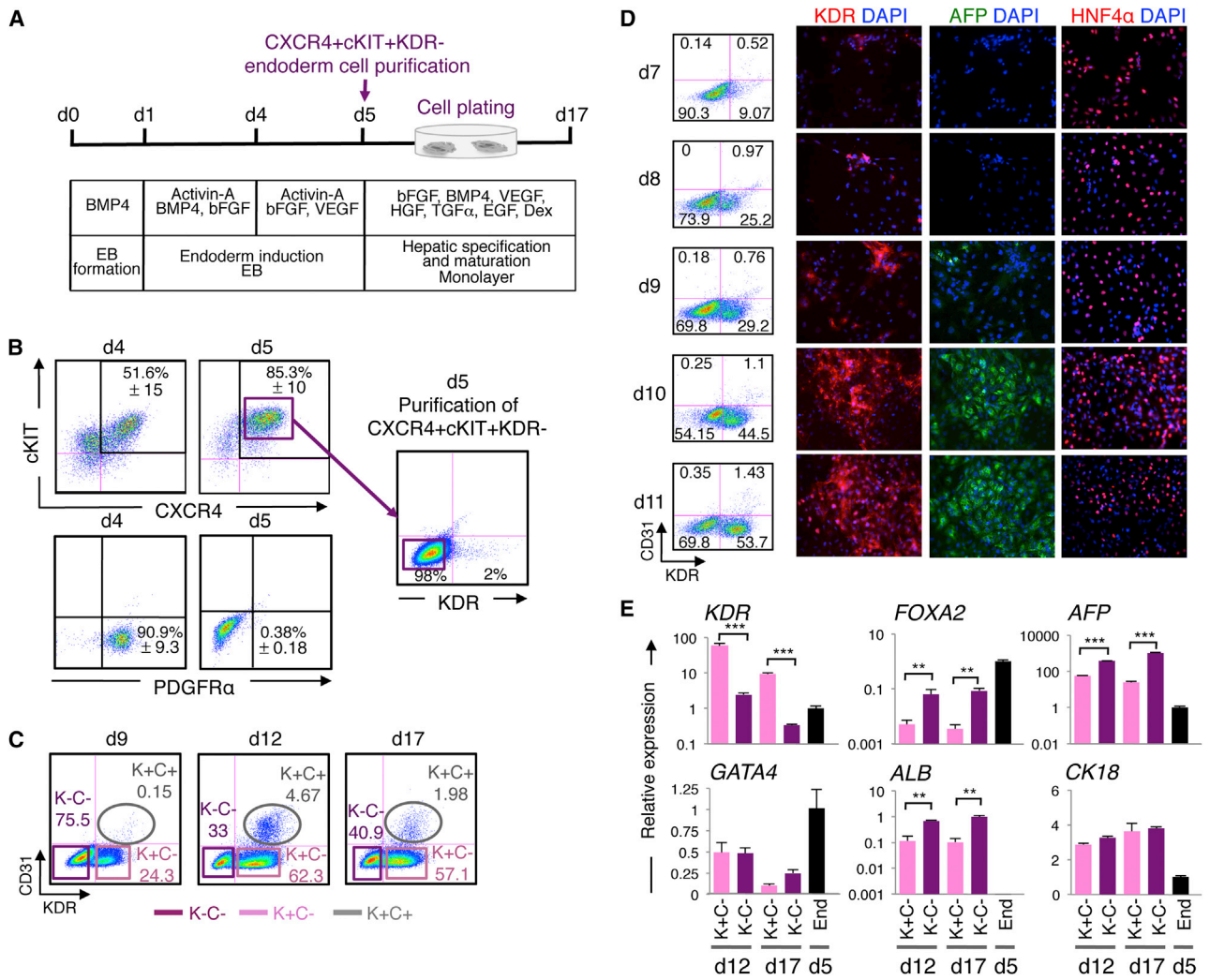


**Figure 1. Concomitant Development of KDR–CD31– Hepatic Cells, KDR+CD31– Prehepatic Cells and KDR+CD31+ Endothelial Cells in hESC-Derived Hepatic Cultures**

(A) hESC hepatic differentiation protocol.

(B) Flow cytometry analyses from day 4 and day 5 (d4 and d5) EBs. Numbers reflect means ± SD for 15 experiments (n = 15) for CXCR4 and cKIT, and n = 3 for PDGFRα.

(C and D) Flow cytometry analyses (C) and immunostainings (D) from hepatic cultures generated from the plated day 5 CXCR4+cKIT+KDR− cells at different time points (×200).

(E) Relative transcript levels in K+C− and K−C− populations purified from day 12 and 17 hepatic cultures. Gene expressions from day 5 CXCR4+cKIT+KDR− cells (d5 "End") were set to 1, except for ALB expression, for which the day 17 isolated K−C− cells were set to 1. Data are represented as mean ± SD (n = 4). See also Figures S1, S2, S3, and S4.

S3A and S3B). Cocultures were analyzed by flow cytometry for KDR and CD31 expression at days 11, 13, and 15 of differentiation, looking for the emergence of K+C− cells that could be explained by fusion between the two cell types. Even after 6 days of coculture, no K+C− cells developed. Moreover, all cells expressing KDR coexpressed CD31 (Figure S3B), confirming the absence of K+C− cells in these cocultures. The second strategy tested whether fusion between K−C− cells and K+C+ cells can occur as the two cell types develop together (Figure S3C). Therefore, purified day 5 endoderm cell populations from the H9-GFP line (constitutively expressing GFP) or from the H9-DsRed line (constitutively expressing DsRed) were cultured together, and the origin of the K+C− cells was examined as they arose (from the H9-GFP or H9-DsRed line if there was no fusion, or from both H9-GFP and H9-DsRed if there was fusion). These data determined that at day 9 of differentiation, when the K+C− population was the largest (for both sets of endoderm populations), the K+C− cells expressed either GFP or DsRed, but never both. In summary, we provide strong evidence that cell fusion between K+C+ endothelial cells and K−C− hepatic cells is not a mechanism responsible for the generation of K+C− cells. Instead, we propose, based on experiments described below, that they are a hepatic precursor population derived from CXCR4+cKIT+KDR− endoderm cells.

To further characterize the K+C− and K−C− populations, cells were purified at day 9, cytospun, and immunostained for KDR, FOXA2, AFP, and CK18. All sorted cell populations contained a purity greater than 97% (Figure S4A). The presence of KDR in K+C− cells and its absence in K−C− cells were confirmed (Figure S4B). Both populations expressed CK18 and the endoderm marker FOXA2, even though levels of FOXA2 were much higher in K−C− cells. However, the hepatic protein AFP was exclusively expressed in K−C− cells at this early time point. Protein expression for these markers was consistent with the transcript levels analyzed by qPCR in K+C− and K−C− populations purified at two later time points, day 12 and day 17 (Figure 1E). Gene-expression levels were compared to those from the day 5 CXCR4+cKIT+KDR− cells (Figure 1E, d5 "End"). The *KDR* transcript levels reflected the protein levels assessed by flow cytometry. The transcript levels of the endoderm marker *FOXA2* and the hepatic markers *AFP* and *ALB* were higher in K−C− cells compared to those in K+C− cells at both time points (24-fold for *FOXA2*, 42.5-fold for *AFP*, and 10-fold for *ALB* at day 17). However, these levels were much higher in K+C− cells than in day 5 CXCR4+cKIT+KDR− cells (24.6-fold for *AFP* and 150-fold for *ALB* at day 17), indicating that K+C− cells progressed to an intermediate hepatic fate. In addition, levels of the ventral endoderm marker *GATA4* (Laverriere et al., 1994) and the epithelial hepatic marker *CK18* were similar in both populations, supporting the hepatic endoderm character of both populations.

Overall, these data demonstrate the coemergence of three populations upon hepatic specification of the hESC-derived endoderm: the K−C− hepatic cells, the K+C+ endothelial cells, and the K+C− cells that most likely represent a previously uncharacterized prehepatic precursor population.

## The K+C– Cells Promote KDR-Mediated Hepatic Maturation of the K–C– Cells in a Non-Cell-Autonomous Manner

Given that the K+C− and K−C− cells develop concomitantly, we next asked whether the K+C− cells are supportive in promoting hepatic specification and maturation of the K−C− cells. We first needed to clarify the hepatic fate potential of both K−C− and K+C− purified populations under defined culture conditions. We compared each cell population either cultured separately or upon coculture with a ratio of 50:50 to reflect the proportion of both populations found in hepatic cultures. K+C− and K−C− populations were purified at day 9, cultured separately (Figure S4C) or cocultured (Figure 2A), and their phenotypes were analyzed at day 17. For tracking the fate of each population in coculture conditions, K+C− cells were purified from the HES-2 cultures, whereas the K−C− cells were derived from the HES2-RFP cultures (Figure S4D). Immunostainings indicated that both populations grown either separately (Figure S4C) or cocultured (Figure 2A) did not modify their phenotype. K−C−RFP+ cells maintained expression for AFP, EpCAM, and CK18 in both separate cultures (Figure S4C) and cocultures (Figure 2A). K+C−RFP− cells maintained expression of CK18, whereas expression of EpCAM and AFP proteins was still not detectable in coculture conditions (Figure 2A), even though low levels of *AFP* transcripts were detected at day 17 in these cells (Figure 1E). Immunostaining for FOXA2 in cocultures confirmed high levels of expression in K−C− cells and lower levels in K+C−, as found previously by qPCR (Figure 2A). These stainings indicated that day 9 K+C− cells do not specify to a hepatic fate following further coculture with the day 9 K−C− cells in a monolayer culture system. The monolayer culture is therefore ideal for determining whether the K+C− cells improve the hepatic fate of the K−C− cells without the potential complication of the K+C− population generating cell-autonomously hepatic cells, as this does not occur in monolayer culture.

Indeed, the ratio between the transcript levels found in cocultures (K+C− with K−C−) and K−C− single cultures indicated that K+C− cells highly induced *AFP* and *ALB* levels in cocultured K−C− cells at day 13 (11.5 ± 1.84-fold and 40.3 ± 21.12-fold, respectively), as well as at day 17 (5.3 ± 3.27-fold and 35 ± 12.6-fold, respectively) (Figure 2B). Because of the concomitant development of the endothelial K+C+ cells with the K−C− cells in this study and our previous work indicating that murine endothelial cells constitute a niche for the murine endoderm to specify to a hepatic fate (Han et al., 2011), the ability of the K+C+ cells to improve hepatic specification of the K−C− cells was also tested. Endothelial K+C+ cells were purified from day 9 cultures and further expanded in culture for 7 days prior to coculture with K−C− cells, with a cell ratio of 5% K+C+ cells and 95% K−C− cells to mimic the proportion observed in hepatic cultures. Because this ratio was very small, we also tested a combination of 25% of K+C+ cells with 75% of K−C− cells (data not shown). With both cell ratios, gene-expression analyses showed no change in *AFP* and *ALB* transcripts following coculture of the K−C− cells with the endothelial K+C+ cells (Figure 2B). Thus, in contrast to what was shown to be the case in the mouse ESC system, here the supportive effect on K−C− hepatic specification was not provided by the K+C+ endothelial cells, but instead was provided by the K+C− cells. However, both supportive cell types, endothelial cells in the mouse system and K+C− cells in the human system, express KDR, which we hypothesized may be required for the supportive effects.

To determine whether KDR expressed on K+C− cells mediates the hepatic specification and maturation of K−C− cells, we cultured the day 5 CXCR4+cKIT+KDR− endoderm-enriched population in monolayer in the presence of either a KDR-inhibitory antibody or the small molecule SU5416, a VEGFR2 kinase inhibitor III (Figure 2C). By day 17, blocking KDR function did not affect *AFP* transcript levels but dramatically reduced levels of *ALB* transcripts (45-fold with the KDR antibody and 75-fold with SU5416), reaching the low levels found in day 12 cultures in the absence of KDR inhibition (Figure 2C). The KDR-inhibitory antibody did not significantly alter the proportion of the three K+C+, K+C−, and K−C− populations (data not shown). To analyze the specificity of the inhibitory function of the antibody and the SU5416 on KDR expressed on K+C− cells, the KDR antibody and SU5416 were tested on cells that don't express KDR (the K−C− cells cultured alone), on K−C− cells cocultured with either cells that express KDR but that are not effective (the K+C+ endothelial cells, Figure S4E), or with the effective K+C− cells (Figure 2D). As illustrated in Figure 2B, K−C− cells were purified from day 9 cultures and grown in the presence or absence of KDR antibody or SU5416 alone or cocultured with the purified day 9 K+C− (Figure 2D) or day 9 K+C+ cells

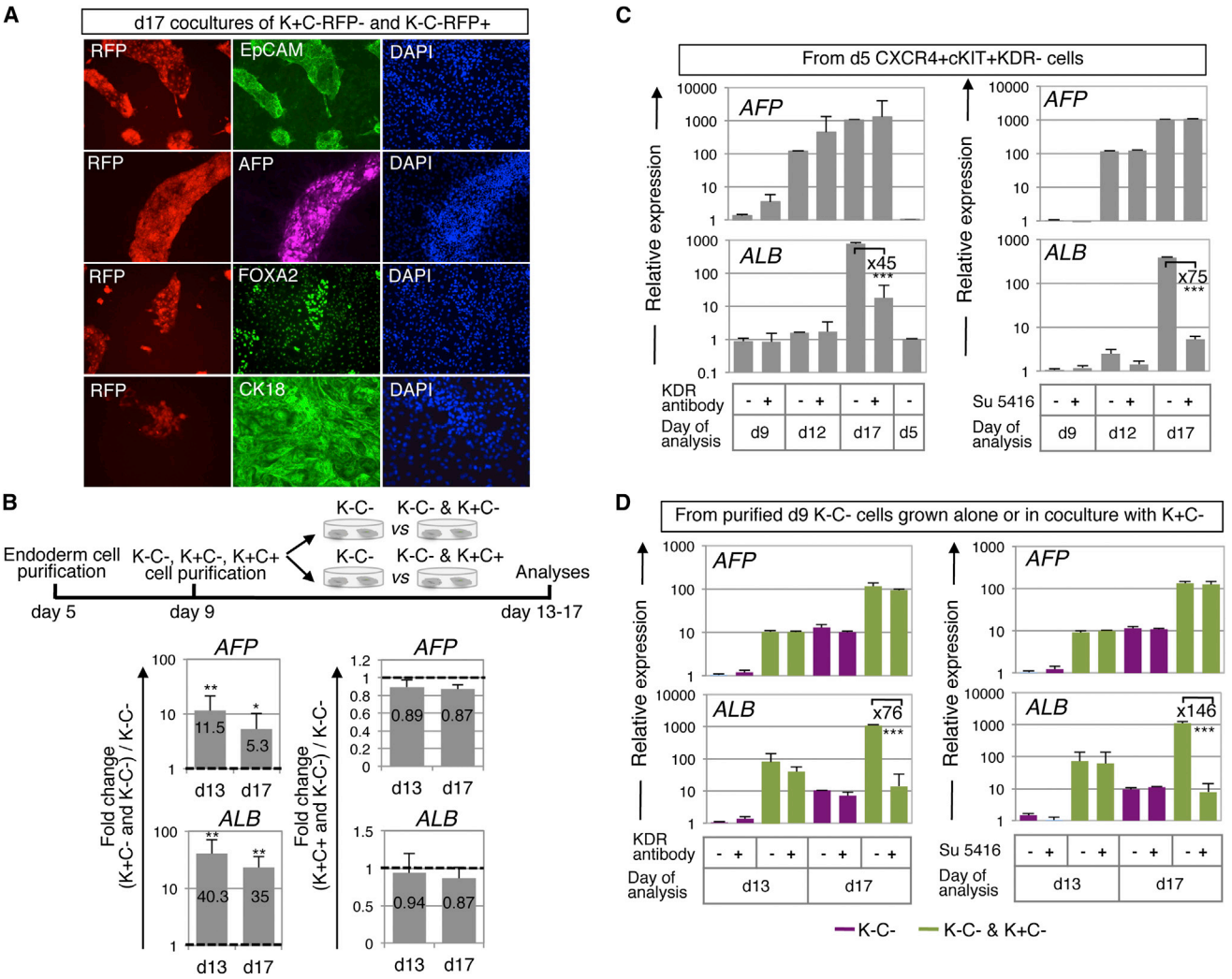


**Figure 2. The K+C– Prehepatic Cells Are Supportive Cells for the Hepatic Maturation of the K–C– Hepatic Cells through KDR**

(A) Immunostainings of day 17 cocultures between the day 9 purified K+C– and day 9 purified K–C– cells (×200).

(B) Illustration of the comparison strategy between K–C– cultured alone with either the coculture K–C– and K+C– (50:50) or with the coculture K–C– and K+C+ (95:5). Graphs represent fold change for transcript levels from the coculture (K–C– and K+C– or K–C– and K+C+) versus K–C– cells cultured alone and harvested at day 13 and day 17 (n = 3 except for *AFP* and *ALB* expression from day 17 K+C– and K–C– versus K–C– for which n = 10).

(C and D) Relative transcript levels in hepatic cultures generated from day 5 CXCR4+cKIT+KDR– cells (C) or from day 9 purified K–C– cells cultured alone (purple columns, D) or cocultured with day 9 purified K+C– (green columns, D) in the presence or absence of a KDR-inhibitory antibody (C and D, left panels) or a small-molecule SU5416 (C and D, right panels). KDR antibody or SU5416 were added to the culture media every 2 days. Transcript levels were set to 1 for the day 5 CXCR4+cKIT+KDR– cell (d5) group (C, left panels), for the day 9 cultures in the presence of DMSO (C, right panels), for the day 13 K–C– single cultures in the presence of IgG isotype control (D, left panels), or for the day 13 K–C– single cultures in the presence of DMSO (D, right panels) (n = 4 for KDR antibody inhibitor and the IgG isotype control, and n = 3 for SU5416 and DMSO control).

(B–D) Data are represented as mean ± SD. *AFP* and *ALB* levels were not significantly different and very similar in the presence of IgG isotype control for KDR or with media alone (data not shown).

See also Figure S4.

(Figure S4E). As expected, *AFP* and *ALB* levels in K–C– cells alone increased from day 13 to day 17 and were not altered by the presence of the KDR-inhibitory antibody nor by SU5416 (Figures 2D and S4E, purple columns). Cocultures of K–C– cells with K+C+ cells (Figure S4E, coculture blue columns) did not improve these levels, confirming the nonsupportive role of K+C+ cells on K–C– cell hepatic fate. In contrast, cocultures of K–C– cells with K+C– cells (Figure 2D, coculture green columns) induced *AFP* and *ALB* levels at both day 13 and day 17 time points. KDR-inhibitory antibody or SU5416 in cocultures abrogated the *ALB* increase induced by the coculture seen at the later time point, day 17 (a 76-fold and 146-fold decrease, respectively), indicating that KDR expressed on K+C– cells mostly controls hepatic maturation (*ALB* levels), but not specification (*AFP* levels), of the K–C– cells.

Our findings demonstrate that K–C– maturation is supported in a non-cell-autonomous manner, dependent on active KDR signaling in the K+C– population.

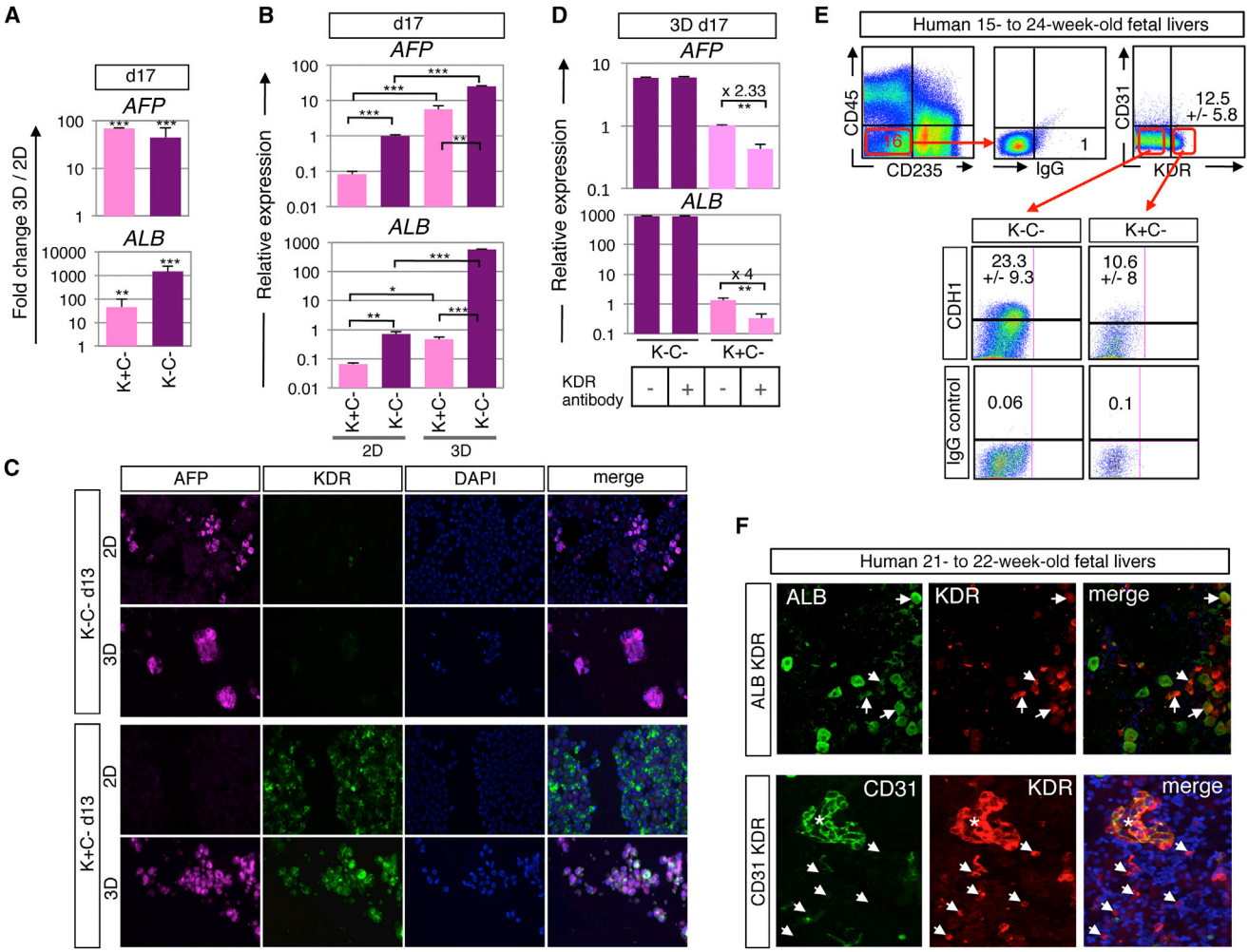


**Figure 3. The hESC-Derived K+C– Cells Are Hepatic Progenitors**

(A) Fold change for transcript levels of the ratio of three-dimensional relative to two-dimensional cultures (3D/2D) from day 9 purified K+C− or K−C− populations, analyzed at day 17 (n = 3).

(B) Relative transcript levels from purified day 9 K+C− and K−C− cells grown either in 2D or in 3D and analyzed at day 17 (n = 4). *AFP* and *ALB* levels were set to 1 for K−C− cells.

(C) Immunocytostainings of the cytospun day 9 purified K+C− and K−C− cells grown for 4 days either in 3D or in 2D (×200). One representative experiment out of two is shown.

(D) Relative transcript levels in day 9 K+C− and K−C− cells grown in 3D in the presence or absence of KDR-inhibitory antibody and analyzed at day 17 (n = 3). Transcript levels were set to 1 for K+C− cells in the absence of KDR antibody (the controls used media alone).

(E) Flow cytometry analyses from 15- to 24-week-old human fetal liver preparations (n = 4).

(F) Immunocytostainings of dissociated and cytospun 21- to 22-week-old human fetal livers (×200).

(A, B, D, and E) Data are represented as mean ± SD.

See also Figure S5.

## The K+C– Cells Can Differentiate into Hepatic Cells

In addition to the supportive function of the K+C− cells, we next examined whether the K+C− cells represent a pool of progenitors for hepatic cells. Although this was not seen in monolayer (2D) cultures, in an attempt to induce hepatic specification of the K+C− cells, purified day 9 populations were cultured in 3D structures (3D aggregates) (Figure 3), which often favor hepatic cell lineage maturation (Han et al., 2012). Day 9 K+C− cells formed large and compact aggregates, whereas the aggregates from day 9 K−C− cells remained small (Figure S5A). Hepatic specification and maturation in 3D were dramatically induced by day 17 in both populations compared to those in 2D, indicated by increased levels of *AFP* (98 ± 2.47-fold in K+C− cells; 87 ± 26.9-fold in K−C− cells) and *ALB* (68 ± 40.25-fold in K+C− cells; 1,200 ± 186-fold in K−C− cells) (Figure 3A). Analyses of *AFP* and *ALB* transcripts at day 17 showed higher levels of *AFP* and similar levels of *ALB* in K+C− 3D cultures compared to the hepatic K−C− 2D cultures, indicating hepatic specification of the K+C− cells in 3D (Figure 3B). Hepatic specification of the K+C− cells was confirmed at the AFP protein level, as most of the K+C− cells cultured in 3D expressed AFP (Figures 3C and S5B, 3D cultures). In 2D cultures, AFP protein was never

detected in K+C− cells, whereas it was consistently seen in some K−C− cells (Figures 3C and S5B, 2D cultures). AFP expression was dramatically increased in K−C− cells cultured in 3D, in that all cells expressed AFP (Figures 3C and S5B, 3D cultures). 3D cultures not only induced hepatic fate of the K+C− progenitors but also improved hepatic maturation of the K−C− hepatic cells. Although numerous studies using human pluripotent stem cells have shown efficient hepatic differentiation in monolayer culture, none investigated the fate of progenitors (endoderm and hepatic progenitors) following cell purification prior to subsequent culture, experimental conditions that greatly impact the cell's capacity to specify efficiently in monolayer. It was thus not surprising that 3D culture was required for specification and maturation of the purified K+C− progenitors. Importantly, we tested whether the hepatic fate of K+C− cells in aggregates was mediated through KDR. Purified day 9 K+C− cells, as well as the day 9 K−C− cells, were aggregated in the absence and presence of KDR-inhibitory antibody until day 17. As expected, KDR inhibition did not affect *AFP* and *ALB* levels in K−C− aggregates, but significantly reduced *AFP* (2.33-fold) and *ALB* (4-fold) levels in K+C− 3D cultures (Figure 3D).

This data further confirmed the specificity of the KDR-inhibitory antibody and indicated that hepatic specification and maturation induced by the 3D cultures of K+C− cells is mediated through KDR in a cell-autonomous manner. Furthermore, these results demonstrate the hepatic potential of the K+C− cells in a 3D culture context that is likely to better recapitulate the cell-cell interactions that occur during liver development.

## Identification of a Similar K+C– Cell Population in Human Fetal Livers

Human fetal livers from 15- to 24-week-old fetuses were dissociated into single-cell suspensions and analyzed via flow cytometry for KDR and CD31 expression (Figure 3E). For exclusion of the blood cells that constitute the majority of the fetal liver (Migliaccio et al., 1986), cells were immunostained with the leukocyte marker CD45, as well as the erythroid marker CD235a. The negative cells for both hematopoietic markers (about 16% of total cells) were gated and analyzed for KDR and CD31 expression (Figure 3E). Even though the fetal livers examined were staged beyond the developmental stages analyzed in hESC cultures, a substantial cell population of the nonhematopoietic cells (12% ± 5.8%) was identified as K+C−, a phenotype reminiscent of the K+C− hESC-derived hepatic progenitors. A fraction of the K+C− cells expressed the known marker for human fetal hepatic progenitor, CDH1 (Terrace et al., 2007), as assessed by flow cytometry (10.6% ± 8%), and low levels of ALB (Schmelzer et al., 2007), assessed by identification of KDR+ALB+ cells following costaining on cytospun cell preparation (Figures 3F, arrows, and S5C). CDH1 was found to be expressed in both the K+C− and K−C− fractions. This was not surprising, given that K+C− cells most likely constitute only a subset of the hepatic progenitor pool, the other progenitors being K−C−. Many KDR+ cells coexpressed CD31, mostly defining the endothelial cell lineage (Figure 3F, area with an asterisk). However, some KDR+ cells excluded CD31 expression (Figure 3F, arrows), supporting the existence of the K+C− population detected by flow cytometry, which may represent the KDR+ALB$^{lo}$ cells. To confirm the immunostaining of cytospun liver cell suspensions, sections of 22-week-old fetal livers were also immunostained for the same markers and examined with a confocal microscope using images of 0.25 μm depth (Figures S5D–S5F). Arrows indicate KDR+ cells coexpressing the hepatic marker ALB (Figures S5D and S5F), as well as some KDR+ cells that exclude the endothelial marker CD31 (Figures S5E and S5F) and hence may represent the hepatic progenitors.

Altogether, analyses of early human fetal livers identified a similar K+C− cell population expressing markers for hepatic progenitors (CDH1 and low levels of ALB), suggesting that some KDR+ cells represent an intermediate hepatic progenitor in human fetal livers, as found in hESC differentiation cultures.

## The hESC-Derived K+C– Hepatic Progenitors Support the HCV Life Cycle following Hepatic Specification and Maturation

To functionally evaluate hepatic progenitor cells, we tested their ability to support infection and replication of HCV, which are features unique to bona fide hepatocytes (Shulla and Randall, 2012). We determined the ability of the K+C− cells to support HCV infection either in 2D cultures, which maintain their progenitor characteristics, or in 3D cultures following hepatic specification and maturation. For comparison, the hepatic functionality of the counterpart K−C− hepatic cells, cultured either in 2D or 3D, as well as the day 13 hepatic differentiation cultures (Hep-hESC), were analyzed similarly (Figure 4A). Cells were challenged with infectious HCV particles that are capable of both entering and replicating in permissive host cells (Figures 4A–4C). Quantification of viral RNA replication over time by qPCR in cells (Figure 4B) or secreted in cell supernatants (Figure 4C) following infection revealed that K+C− cells cultured in 2D were poorly infected, whereas K+C− cells cultured in 3D supported efficient HCV RNA replication (Figure 4B, 25-fold induction; Figure 4C, 51-fold induction) to levels equivalent to those observed in hepatic K−C− cells (in either 2D or 3D) or in Hep-hESC. The increase in signal was dependent on authentic HCV RNA replication mechanisms, because the HCV RNA polymerase inhibitor 2′C-methyl-adenosine (2′CMA, Figures 4B and 4C) prevented RNA amplification over time. This replication was extremely efficient; RNA levels were comparable to those observed in parallel infections of human hepatoma-derived Huh-7.5 cells (Figures 4B and 4C), which are more susceptible to HCV infection than any other known cell line. Thus, an infection that approaches the levels observed in Huh-7.5 cells should be considered compelling. Furthermore, the HCV RNA secreted by K+C− cells (in 3D only), K−C− cells (in either 2D or 3D), or Hep-hESC was validated to represent newly produced infectious virus by titering on naive Huh-7.5 cells (Figure 4D, tissue culture infectious doses 50% per ml [TCID50/ml]). Indeed, levels of infectious-virus release from 3D K+C− cells (3D only), K−C− cells (in either 2D or 3D), or Hep-hESC were similar and approaching those in Huh-7.5 cells.

Thus Hep-hESC, K−C− hepatic cells, and the K+C− cells that are further specified and matured in 3D culture conditions all support the entire HCV life cycle nearly as efficiently as the best-case Huh-7.5 cells. Therefore, the K+C− cells are true progenitors that derive functional hepatic cells.

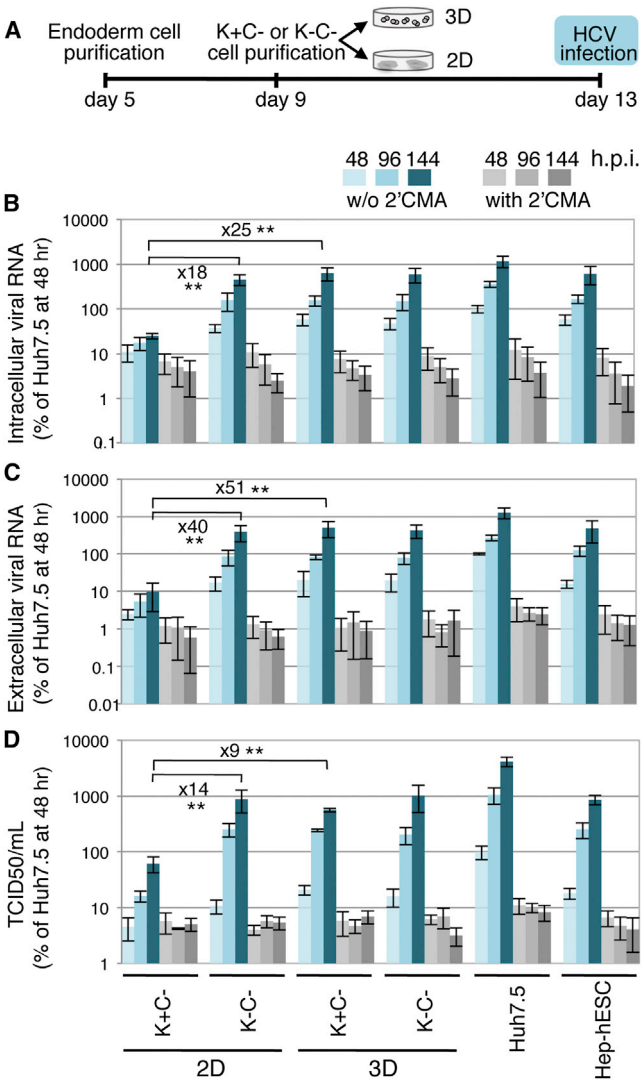


**Figure 4. K+C– Hepatic Progenitors Support HCV Infection following Specification and Maturation**

(A) Illustration of the HCV infection protocol. Cell populations infected with HCV were the day 9 purified K+C− or K−C− cells further cultured in 2D or 3D for 4 more days (until day 13), the day 13 hepatic cultures (Hep-hESC that includes both K−C− and K+C− cells), and the highly HCV-permissive Huh7.5 cells. For the 3D cultures, floating aggregates were plated onto matrigel the day before infection. All cell populations were infected at day 13 of differentiation.

(B) Intracellular HCV RNA was quantified by qPCR at the indicated time points, either in the absence (blue columns) or presence (gray columns) of 2′CMA.

(C) HCV RNA released from supernatants of the above infections was quantified by qPCR.

(D) Infectious virus in these supernatants was quantified with a limiting dilution assay on Huh7.5 cells and represented by the TCID50/ml. 2′CMA controls for the presence of input HCV RNA derived from particles introduced during infection. For (B–D), values are normalized to Huh7.5 readings at 48 hr post infection (h.p.i.) and represent means ± SD of two independent experiments, each performed in triplicate. **p < 0.01, ***p < 0.001 (Mann-Whitney test).

## KDR+ Progenitors Contribute to Early Hepatic Endoderm and Hepatoblast Development In Vivo

In order to provide in vivo evidence for the existence of a KDR-expressing hepatic progenitor, mouse embryos from embryonic day 8.0 (E8.0) (prior to hepatic specification), E8.5 (hepatic endoderm stage), E9.5 (liver bud stage), and E13.5 (fetal livers) were examined for expression of KDR and the endoderm marker FOXA2 by immunostaining. Few KDR+FOXA2+ cells were detected in foregut endoderm and were only found in E8.0 embryos prior to hepatic specification (Figure 5A, arrows indicating two KDR+FOXA2+ cells). To demonstrate the in vivo contribution of KDR+FOXA2+ endoderm cells to the hepatic lineage, we used a *Kdr* lineage-tracing mouse model. This mouse model is a cross between the heterozygous *Kdr-Cre* mouse, in which the *Cre* recombinase gene was knocked into the *Kdr* locus (Motoike et al., 2003), and the homozygous reporter enhanced YFP mouse, in which YFP is ubiquitously expressed under the *Rosa26* promoter, after Cre recombinase excises the *STOP* cassette flanked by LoxP sites (Srinivas et al., 2001). This well-established and validated model has been used extensively by other groups to track early progenitors for hematopoietic cells (Lugus et al., 2009) and endothelial cells (Coveney et al., 2008; Lavine et al., 2006; White et al., 2007). The *Kdr-Cre* line is a *Cre* knockin into the first exon of the *Kdr* gene, faithfully expressing KDR, as was validated after crossing with the *Rosa26*-$^{Loxp}$STOP$^{Loxp}$LacZ line (Motoike et al., 2003). The resulting offspring include 50% of the mice carrying the lineage tracer (hereafter YFP$^{pos}$ mice) and 50% of the mice without YFP+ cells, used as a negative control (hereafter YFP$^{neg}$ mice). The YFP$^{pos}$ mice allow tracking of not only cells expressing KDR, but also descendant cells that subsequently downregulate KDR expression.

To evaluate the KDR cell-lineage tracing efficiency in the YFP$^{pos}$ mice, trunks of E10.5 embryos (whole embryos with the exclusion of limbs, head, and tail) and E13.5 fetal livers were dissociated and analyzed by flow cytometry for KDR expression and YFP fluorescence (Figure S6A). Data pooled from either 11 E10.5 embryos or 36 E13.5 fetal livers indicated that 57.3% ± 8.6% or 40% ± 15.1% of KDR+ cells coexpressed YFP, respectively (Figure S6A). The progeny of KDR+ cells found at these early time points include endothelial cells and the primitive hematopoietic cells that represent about 90% of the cells in E13.5 fetal livers. To specifically assess the lineage-tracing efficiency for tracking endothelial cells, we performed similar flow cytometry analyses using the endothelial marker CD31 (Figure S6B). We found that 79.4% ± 10.9% (n = 11, E10.5 embryos) and 72.8% ± 9.5% (n = 36, E13.5 fetal livers) of CD31+ cells costained with YFP.

Next, we utilized the YFP$^{pos}$ mice to investigate the existence of YFP+ progeny in the hepatocytic lineage. The presence of single YFP+ cells was detected in two out of seven embryos as early as E8.5 in the foregut hepatic endoderm, as indicated by single cells coexpressing YFP and the endoderm marker FOXA2 (Figures 5B, arrow, and S6C). However, this may be a minimal estimate, because cells may have been missed due to technical issues concerning the fragility of consecutive sections of the foregut endoderm, which made it very challenging to screen the entire foregut of each embryo. One day later, in E9.5 embryos, many YFP+ cells coexpressing FOXA2 were found in the developing liver bud (Figures 5C, arrows, and S6D). The identity of the liver bud was confirmed by costaining for FOXA2 and AFP on successive sections (Figure 5D, top panel), and the identity of the YFP hepatoblasts was confirmed with a costaining for AFP and YFP (Figure 5D, bottom panel, arrows). The contribution of the

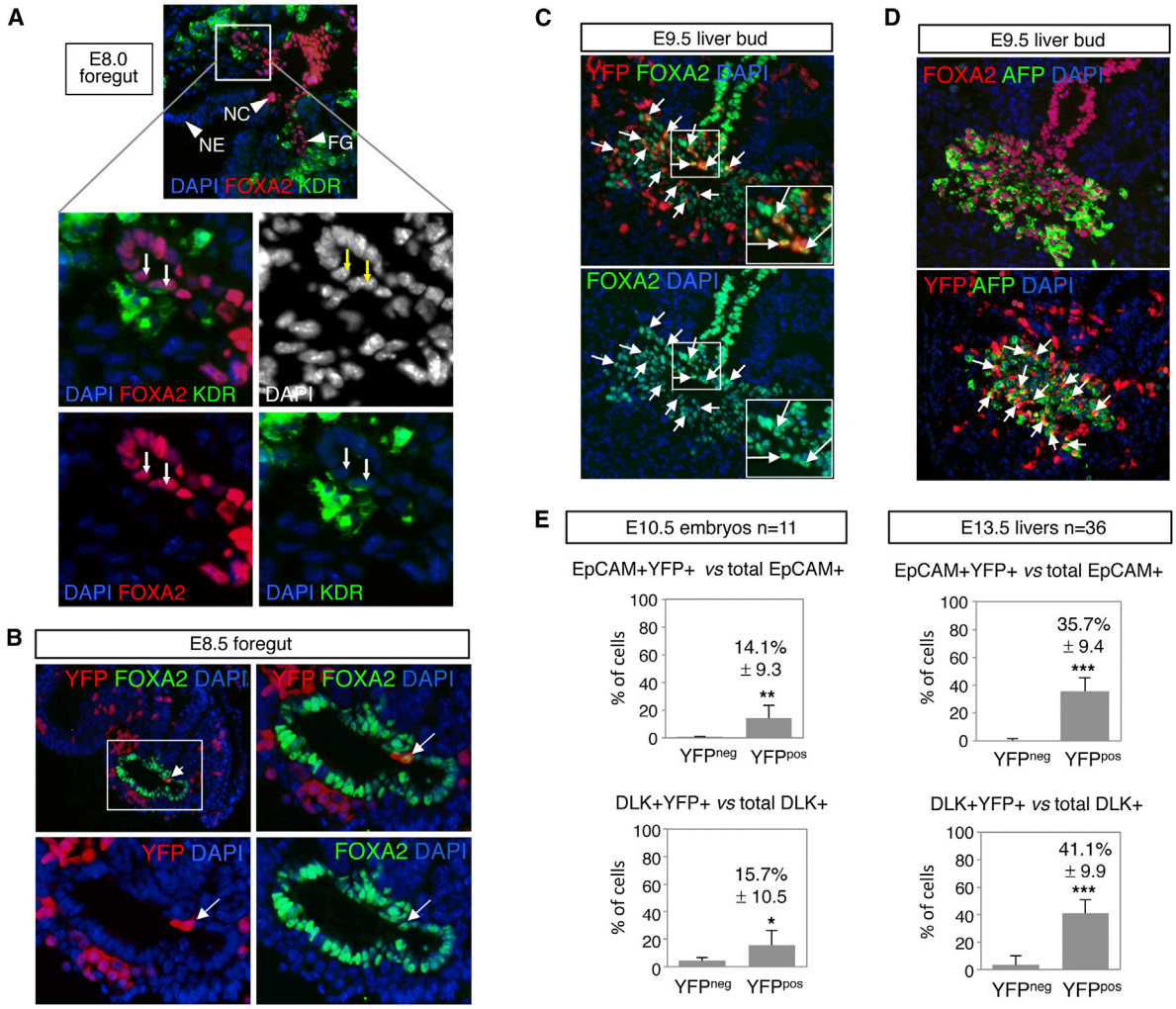


**Figure 5. KDR+ Progenitors Contribute to the Development of Hepatic Endoderm and Fetal Hepatoblasts during Mouse Embryogenesis**

(A) Immunostaining of E8.0 foregut endoderm sections from $YFP^{pos}$ mice (×100 for the upper panel; ×200 for the four other panels that are the close-up pictures of the upper panel). FG, foregut diverticulum; NC, notochord; NE, neuroepithelium.

(B) Immunostaining of E8.5 foregut endoderm sections from $YFP^{pos}$ mice. The upper left panel represents a low magnification view (×100), whereas the three other panels are close-up pictures of the framed field (×200).

(C and D) Immunostaining of E9.5 liver bud sections from $YFP^{pos}$ mice (×200). Insets represent close-up pictures.

(E) Graphs indicate the means ± SD of the percentages of YFP+EpCAM+ cells over the whole EpCAM+ cell population or the percentage of YFP+DLK+ cells over the whole DLK+ cell population obtained by flow cytometry analyses from 11 trunks of E10.5 embryos and 36 E13.5 fetal livers.

See also Figures S6 and S7.

KDR+ progenitor cells to the hepatoblast population was quantified in trunks of E10.5 embryos and E13.5 fetal livers by flow cytometry for YFP and two specific markers for hepatoblasts, delta-like 1 homolog (DLK)/Pref-1 and the epithelial cell adhesion molecule (EpCAM). DLK is strongly and specifically expressed in hepatoblasts from E10.5 to E14.5 embryos (Tanimizu et al., 2003). Similarly, EpCAM is a specific marker for endoderm derivatives in E9.5 embryos, including hepatoblasts of the liver bud (Sherwood et al., 2007), and is also expressed homogenously in all hepatoblasts until E14.5 (Tanaka et al., 2009). Flow cytometry analyses of dissociated E10.5 trunks (from 11 embryos) and E13.5 fetal livers (from 36 livers) indicated that the percentages of cells positive for EpCAM or DLK coexpressing YFP were similar (~15% in E10.5 trunks and ~40% in E13.5 fetal livers, Figures 5E and S6E). The identity of the YFP+ hepatoblasts was confirmed by coimmunostaining for YFP and AFP on sections (Figures S7A, arrows, and S7B) from E10.5 embryos and E13.5 fetal livers. Percentages of hepatoblasts in E13.5 fetal livers ranged between 3% and 4% of the whole liver cell population based on DLK and EpCAM expression and were consistent with previous studies using the same markers, as well as the hepatoblast markers Liv-2 and E-cadherin (Nierhoff et al., 2005; Tanaka et al., 2009; Tanimizu et al., 2003). It is noteworthy that all fetal livers analyzed (from n = 36 embryos) were consistently composed of a large population of YFP+ hepatoblasts ranging from 30% to 50%

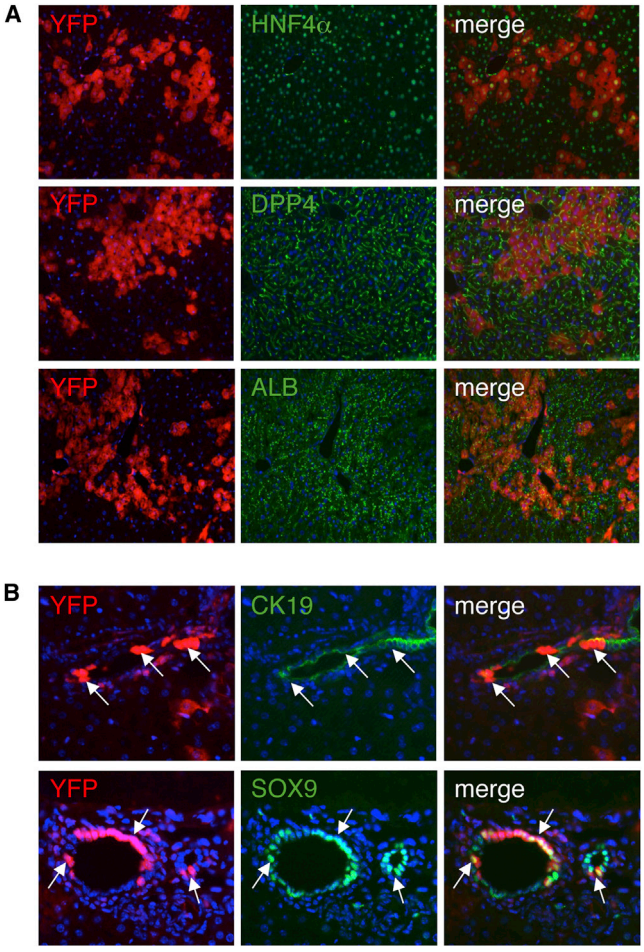


**Figure 6. KDR+ Progenitors Contribute to the Development of Adult Hepatocytes and Cholangiocytes**

(A and B) Immunostaining on liver sections of 5-week-old YFP$^{pos}$ mice (×200). See also Figure S7.

of the total hepatoblast population, indicating that the contribution of a KDR+ progenitor to hepatoblast development is not a random event due to leaky Cre expression but rather occurs consistently and robustly in all embryos.

Altogether, analyses of fetal liver development from the E8.0 hepatic endoderm to the E13.5 fetal liver demonstrated a progressive and robust contribution in all embryos analyzed of the KDR+YFP+ progenitors to hepatoblast development, including up to 50% of the hepatoblast population at E13.5. Given that the tracing of endothelial cells showed efficiency for Cre at approximately 75%, this number probably represents an underestimate of the true contribution of KDR+ progenitor cells to hepatoblasts.

### KDR+ Progenitors Contribute to Adult Hepatocyte and Cholangiocyte Development In Vivo

Since the hepatoblast represents a common progenitor for the adult hepatocyte and cholangiocyte, we investigated whether the KDR+ cell-derived YFP+ hepatoblasts found in fetal livers gave rise to adult YFP+ hepatocytes and YFP+ cholangiocytes (Figure 6). Immunostainings of livers from adult YFP$^{pos}$ mice revealed the presence of a large population of YFP+ hepatocytes easily recognizable by their cuboidal shape (Figures 6A and S7C). All YFP+ hepatocytes coexpressed hepatocyte markers including HNF4α; dipeptidyl peptidase-4 (DPP4), which marks the bile canaliculi at the membrane of hepatocytes; or ALB (Figures 6A, S7C, and S7D). In contrast to the robust contribution of KDR+ progenitors to fetal hepatoblast development, the percentage of YFP+ hepatocytes in adult mice varies from mouse to mouse and from lobe to lobe within the same mouse between ~1% and ~40%, as shown in Figure S7E. Careful examination of the distribution of YFP hepatocytes among many adult livers did not reveal any specific preferential location in pericentral or periportal regions. Some YFP+ cells also marked cholangiocytes that were identified by expression for CK19 and SOX9 (Antoniou et al., 2009) (Figures 6B, arrows, and S7D). This variable contribution suggests that adult YFP+ hepatocytes and YFP+ cholangiocytes are replaced over time after birth from YFP− progenitor cells. As expected, most of the endothelial cells were also YFP+ in adult livers (Figure S7F). The variability in detecting endothelial cells with YFP staining on sections in adult liver was solely due to the level of exposure used. Hepatocytes are such large cells in comparison to the very thin endothelial cells that it was technically difficult to visualize both of them with the same exposure. When the exposure is increased, it is obvious that most of the endothelial cells also stain positive for YFP.

Altogether, the KDR lineage-tracing study provides in vivo evidence for the existence of a KDR+ hepatic progenitor that contributes robustly to the development of a large subset of fetal hepatoblasts that in turn differentiate into adult hepatocytes and cholangiocytes.

## DISCUSSION

Hepatocyte transplantation for the treatment of liver diseases has been proposed as a bridge for whole-organ transplantation, because there is a severe shortage of liver donors. The field of pluripotent stem cell differentiation has the potential to provide a ready and unlimited source for transplantable hepatocytes. The goal of this study was to uncover the early cellular events and mechanisms that support the development of hESC-derived hepatic cells. This study revealed an early hepatic progenitor defined as a cell expressing KDR that constitutes a pool of hepatic progenitors and supportive cells for the committed hepatic cells. The present study reveals that KDR expression unexpectedly marks an endoderm lineage progenitor which is a hepatic progenitor.

The K+C− human hepatic progenitors defined in this study share some characteristics with previously described hepatocyte progenitors from human fetal livers. Multiple markers have been utilized for isolating human fetal progenitors, reflecting in part the different ages of the fetal livers analyzed. In the earliest stages (before 10 weeks), most studies describe bipotent liver progenitors that express markers such as CD117, CD34, and CD90 (Nava et al., 2005; Nowak et al., 2005; Nyamath et al., 2007). However, human hepatoblasts with classic hepatobiliary phenotype, characterized by the expression of EpCAM, CK8/18, AFP, ALB, and CK19 were isolated from the livers at a later stage (Mahieu-Caputo et al., 2004; Schmelzer et al., 2006). The

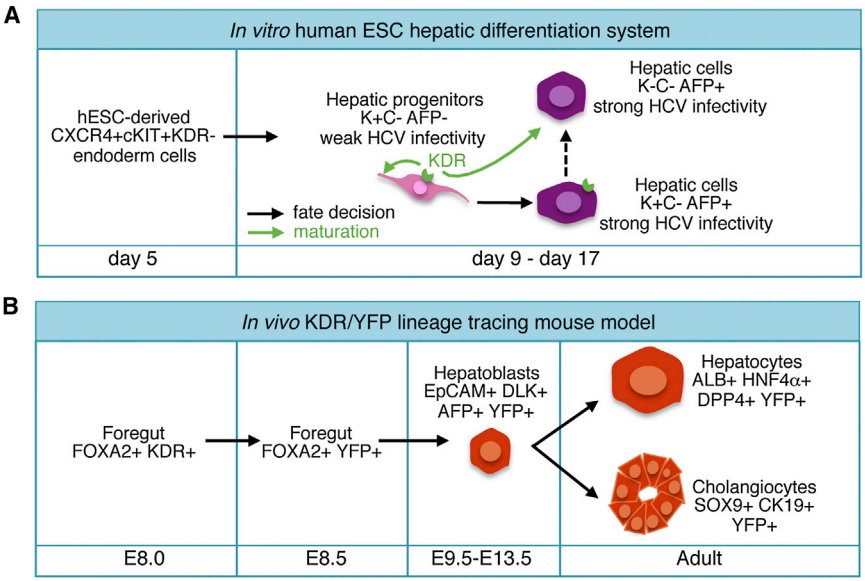


**Figure 7. Identification and Function of the KDR Hepatic Progenitor Using the In Vitro hESC System and an In Vivo KDR/YFP Lineage-Tracing Mouse Model**

(A) The in vitro hESC system.

(B) An in vivo KDR/YFP lineage-tracing mouse model.

K+C− progenitor cells established in this study most likely represent an intermediate hepatic progenitor that expresses CK18 but is negative for AFP, ALB, and EpCAM in vitro. We were able to detect K+C− cells in the developing human fetal liver. The relatively low percentage of K+C− cells in fetal livers (12% ± 5.8% after exclusion of blood cells) compared to the higher percentage found in the hESC differentiation cultures (20% to 65%) is perhaps due to the fact that the K+C− cells develop earlier (before 15 weeks of gestation) and transiently in the fetal liver. Studies of liver development in mice have helped determine the timing of the emergence of liver progenitor cells. To date, all known hepatic progenitor markers defined in the literature identify hepatoblasts (LIV2, DLK/Pref-1, Nope, E-cadherin, cMET, and EpCAM) (Nierhoff et al., 2007; Nitou et al., 2002; Suzuki et al., 2002; Tanaka et al., 2009; Tanimizu et al., 2003) or stem cell-like cells as emerging when the fetal hepatoblast determines either a hepatocytic or cholangiocytic fate. Stem cell-like cells are localized in the developing portal track in E14.5–E16.5 embryos and are identified by expression of SOX9 (Furuyama et al., 2011). Stem cell-like cells are also found as dormant cells in adult livers in the portal track area, and they contribute to liver regeneration in the case of severe injury (SOX9, FOXL1, EpCAM, and LGR5) (Dorrell et al., 2011; Furuyama et al., 2011; Huch et al., 2013; Okabe et al., 2009; Sackett et al., 2009). In contrast to these studies, the previously unreported KDR+ hepatic progenitor uncovered in the present study appears in the endoderm before the hepatoblast stage, characterizing it as a progenitor for the hepatoblast.

We provide evidence that the K+C− cells are not only hepatic progenitors but also support the maturation of K−C− hepatic cells, mediated indirectly through the KDR receptor, and that this supportive effect is not promoted by the other hepatic cell niche component, the K+C+ endothelial cells. This was intriguing, in that several groups including ours have shown the supportive function of endothelial cells in promoting hepatic specification and expansion of the hepatic endoderm in early mouse liver development (Han et al., 2011; Matsumoto et al., 2001) and in promoting mouse liver regeneration (Ding et al., 2010). The discrepancy of the role of endothelial cells in liver development between the mouse and human systems may be due to the different timing of appearance of the supportive progenitor cells in both species. In the mouse, the KDR progenitors are transient cells found in the foregut endoderm no later than E8.0, suggesting a possible role for the progenitors in hepatic specification of endoderm, but most likely not in hepatic endoderm expansion, as shown previously for endothelial cells. In contrast, in hESC hepatic differentiation cultures, the KDR progenitors develop prior to endothelial cells and in parallel to hepatic cells, and they remain for days. Their persistent concomitant presence with the developing hepatic cells may explain their critical role in hepatic specification and maturation, compared to endothelial cells. Nevertheless, both cell types, progenitors and endothelial cells, have a common feature; they both express KDR. Absence of KDR correlated with a lack of endothelial cells in *Kdr*$^{-/-}$ mice led to reduced *ALB* transcript levels in liver bud transplants (Matsumoto et al., 2001). Similarly, inhibition of KDR expressed on hepatic progenitors in hESC hepatic cultures blocked *ALB* transcript induction. Even though the supportive cells are different in the two systems, they seem to both act through the same KDR receptor to regulate hepatic maturation.

In summary, using the hESC system, we define a hepatic niche in which the K−C− committed hepatic cells (AFP+ALB+) develop concomitantly with the K+C− hepatic progenitors (AFP−ALB−) (Figure 7A). The K+C− progenitors can differentiate through a KDR-mediated mechanism into hepatic cells (KDR+AFP+) that are functional, given that they support HCV pathogenesis and presumably transition by downregulating KDR to generate the typical K−C−AFP+ hepatic cells. The K+C− progenitors are also supportive cells for the K−C− committed hepatic cells, improving their maturation through a KDR-mediated mechanism. The identity and function of the K+C− cell as a hepatic progenitor is conserved in the mouse. In the mouse embryo, KDR+ cells are localized in the endoderm in early E8.0 embryos prior to hepatic specification and further specify to hepatoblasts as KDR expression is downregulated. KDR progenitor-derived hepatoblasts in turn give rise to a subset of adult hepatocytes and cholangiocytes (Figure 7B). We demonstrated in this study that KDR, originally defined as a mesodermal marker and functional receptor for vascular and hematopoietic proper development, also marks hepatic endoderm progenitors and functions to instruct early human liver development.

## EXPERIMENTAL PROCEDURES

### hESC Hepatic Differentiation

The day prior to differentiation, hESCs were harvested using accutase and passaged on matrigel to deplete the mouse embryonic fibroblasts (Invitrogen). At day 0 of differentiation, dissociated hESCs were cultured in low cluster plates (Costar) to allow EB formation in serum-free differentiation (SFD) media as previously described (Han et al., 2011), supplemented with BMP4 (3 ng/ml, R&D Systems). At day 1 the medium was changed to SFD media supplemented with Activin A (100 ng/ml, R&D Systems), basic FGF (bFGF, 2.5 ng/ml, R&D Systems), and BMP4 (0.5 ng/ml, R&D Systems). At day 4, the medium was changed to the SFD media supplemented with Activin A (100 ng/ml), bFGF (2.5 ng/ml), and vascular endothelial growth factor (VEGF, 10 ng/ml, R&D Systems). The day 5 EBs were dissociated, and the CXCR4+cKit+KDR− cells were isolated by FACS and subsequently plated on gelatin-coated dishes (50,000 cells per well of a 48-well plate) in hepatic media as previously described (Han et al., 2011). Inhibition of KDR was performed by adding the KDR-neutralizing antibody (40 ng/ml; R&D Systems) or SU5416 (5 μM; Millipore) every other day from the day 6-plated CXCR4+cKIT+KDR− cells or from the day 10-plated K+C−, K−C−, and K+C+ sorted cells. The isotype immunoglobulin G (IgG, 40ng/ml; Jackson ImmunoResearch) or dimethyl sulfoxide (DMSO, 5 μM; Sigma-Aldrich) were added in the media as controls.

### Human Fetal Liver Dissociation

Fetal liver specimens between 15 and 24 weeks' gestation were obtained at the Mount Sinai Medical Center. This study has been approved by the Mount Sinai institutional review board office as non-human-subject research.

### Mice

*Kdr*-Cre, *Rosa26*-EYFP mice were obtained by crossing the *Kdr*-Cre mice (Motoike et al., 2003) with *Rosa26R*-EYFP mice (Srinivas et al., 2001) for visualization of KDR lineage-tracing cells. The use of mouse models in these experiments received Institutional Animal Care and Use Committee approval.

### Statistical Analysis

Results are expressed as mean ± SD. For each group, at least three experiments were analyzed, and different groups were compared using the t test analysis. $p < .05$ was considered statistically significant; *, $p < .05$; **, $p < .01$; and ***, $p < .001$. Additional experimental procedures are listed in Supplemental Experimental Procedures.

## SUPPLEMENTAL INFORMATION

Supplemental Information includes Supplemental Experimental Procedures, seven figures, and three tables and can be found with this article online at http://dx.doi.org/10.1016/j.stem.2013.04.026.

## ACKNOWLEDGMENTS

This work was supported by the Black Family Stem Cell Institute, the National Institute of Diabetes and Digestive and Kidney Diseases for the mouse study (R01DK087867-01 to V.G.E.), the Robin Chemers Neustein Postdoctoral Fellowship (M.S.), the American Cancer Society (RSG-12-176-01-MPC to M.J.E.), and the Pew Charitable Funds (M.J.E.).

Received: March 26, 2012
Revised: August 10, 2012
Accepted: April 29, 2013
Published: June 6, 2013

## REFERENCES

Agarwal, S., Holton, K.L., and Lanza, R. (2008). Efficient differentiation of functional hepatocytes from human embryonic stem cells. Stem Cells *26*, 1117–1127.

Antoniou, A., Raynaud, P., Cordi, S., Zong, Y., Tronche, F., Stanger, B.Z., Jacquemin, P., Pierreux, C.E., Clotman, F., and Lemaigre, F.P. (2009). Intrahepatic bile ducts develop according to a new mode of tubulogenesis regulated by the transcription factor SOX9. Gastroenterology *136*, 2325–2333.

Cai, J., Zhao, Y., Liu, Y., Ye, F., Song, Z., Qin, H., Meng, S., Chen, Y., Zhou, R., Song, X., et al. (2007). Directed differentiation of human embryonic stem cells into functional hepatic cells. Hepatology *45*, 1229–1239.

Coveney, D., Cool, J., Oliver, T., and Capel, B. (2008). Four-dimensional analysis of vascularization during primary development of an organ, the gonad. Proc. Natl. Acad. Sci. USA *105*, 7212–7217.

D'Amour, K.A., Agulnick, A.D., Eliazer, S., Kelly, O.G., Kroon, E., and Baetge, E.E. (2005). Efficient differentiation of human embryonic stem cells to definitive endoderm. Nat. Biotechnol. *23*, 1534–1541.

Ding, B.S., Nolan, D.J., Butler, J.M., James, D., Babazadeh, A.O., Rosenwaks, Z., Mittal, V., Kobayashi, H., Shido, K., Lyden, D., et al. (2010). Inductive angiocrine signals from sinusoidal endothelium are required for liver regeneration. Nature *468*, 310–315.

Dorrell, C., Erker, L., Schug, J., Kopp, J.L., Canaday, P.S., Fox, A.J., Smirnova, O., Duncan, A.W., Finegold, M.J., Sander, M., et al. (2011). Prospective isolation of a bipotential clonogenic liver progenitor cell in adult mice. Genes Dev. *25*, 1193–1203.

Duan, Y., Ma, X., Zou, W., Wang, C., Bahbahan, I.S., Ahuja, T.P., Tolstikov, V., and Zern, M.A. (2010). Differentiation and characterization of metabolically functioning hepatocytes from human embryonic stem cells. Stem Cells *28*, 674–686.

Ema, M., Takahashi, S., and Rossant, J. (2006). Deletion of the selection cassette, but not cis-acting elements, in targeted Flk1-lacZ allele reveals Flk1 expression in multipotent mesodermal progenitors. Blood *107*, 111–117.

Furuyama, K., Kawaguchi, Y., Akiyama, H., Horiguchi, M., Kodama, S., Kuhara, T., Hosokawa, S., Elbahrawy, A., Soeda, T., Koizumi, M., et al. (2011). Continuous cell supply from a Sox9-expressing progenitor zone in adult liver, exocrine pancreas and intestine. Nat. Genet. *43*, 34–41.

Gouon-Evans, V., Boussemart, L., Gadue, P., Nierhoff, D., Koehler, C.I., Kubo, A., Shafritz, D.A., and Keller, G. (2006). BMP-4 is required for hepatic specification of mouse embryonic stem cell-derived definitive endoderm. Nat. Biotechnol. *24*, 1402–1411.

Han, S., Dziedzic, N., Gadue, P., Keller, G.M., and Gouon-Evans, V. (2011). An endothelial cell niche induces hepatic specification through dual repression of Wnt and Notch signaling. Stem Cells *29*, 217–228.

Han, S., Bourdon, A., Hamou, W., Dziedzic, N., Goldman, O., and Gouon-Evans, V. (2012). Generation of functional hepatic cells from pluripotent stem cells. J. Stem Cell Res. Ther. *S10*, 008.

Hannan, N.R., Segeritz, C.P., Touboul, T., and Vallier, L. (2013). Production of hepatocyte-like cells from human pluripotent stem cells. Nat. Protoc. *8*, 430–437.

Hay, D.C., Fletcher, J., Payne, C., Terrace, J.D., Gallagher, R.C., Snoeys, J., Black, J.R., Wojtacha, D., Samuel, K., Hannoun, Z., et al. (2008). Highly efficient differentiation of hESCs to functional hepatic endoderm requires ActivinA and Wnt3a signaling. Proc. Natl. Acad. Sci. USA *105*, 12301–12306.

Holmes, K., Roberts, O.L., Thomas, A.M., and Cross, M.J. (2007). Vascular endothelial growth factor receptor-2: structure, function, intracellular signalling and therapeutic inhibition. Cell. Signal. *19*, 2003–2012.

Huch, M., Dorrell, C., Boj, S.F., van Es, J.H., Li, V.S., van de Wetering, M., Sato, T., Hamer, K., Sasaki, N., Finegold, M.J., et al. (2013). In vitro expansion of single Lgr5+ liver stem cells induced by Wnt-driven regeneration. Nature *494*, 247–250.

Kopper, O., and Benvenisty, N. (2012). Stepwise differentiation of human embryonic stem cells into early endoderm derivatives and their molecular characterization. Stem Cell Res. (Amst.) *8*, 335–345.

Laverriere, A.C., MacNeill, C., Mueller, C., Poelmann, R.E., Burch, J.B., and Evans, T. (1994). GATA-4/5/6, a subfamily of three transcription factors transcribed in developing heart and gut. J. Biol. Chem. *269*, 23177–23184.

Lavine, K.J., White, A.C., Park, C., Smith, C.S., Choi, K., Long, F., Hui, C.C., and Ornitz, D.M. (2006). Fibroblast growth factor signals regulate a wave of Hedgehog activation that is essential for coronary vascular development. Genes Dev. *20*, 1651–1666.

Lugus, J.J., Park, C., Ma, Y.D., and Choi, K. (2009). Both primitive and definitive blood cells are derived from Flk-1+ mesoderm. Blood *113*, 563–566.

Mahieu-Caputo, D., Allain, J.E., Branger, J., Coulomb, A., Delgado, J.P., Andreoletti, M., Mainot, S., Frydman, R., Leboulch, P., Di Santo, J.P., et al. (2004). Repopulation of athymic mouse liver by cryopreserved early human fetal hepatoblasts. Hum. Gene Ther. *15*, 1219–1228.

Matsumoto, K., Yoshitomi, H., Rossant, J., and Zaret, K.S. (2001). Liver organogenesis promoted by endothelial cells prior to vascular function. Science *294*, 559–563.

Migliaccio, G., Migliaccio, A.R., Petti, S., Mavilio, F., Russo, G., Lazzaro, D., Testa, U., Marinucci, M., and Peschle, C. (1986). Human embryonic hemopoiesis. Kinetics of progenitors and precursors underlying the yolk sac——liver transition. J. Clin. Invest. *78*, 51–60.

Motoike, T., Markham, D.W., Rossant, J., and Sato, T.N. (2003). Evidence for novel fate of Flk1+ progenitor: contribution to muscle lineage. Genesis *35*, 153–159.

Nava, S., Westgren, M., Jaksch, M., Tibell, A., Broomé, U., Ericzon, B.G., and Sumitran-Holgersson, S. (2005). Characterization of cells in the developing human liver. Differentiation *73*, 249–260.

Nierhoff, D., Ogawa, A., Oertel, M., Chen, Y.Q., and Shafritz, D.A. (2005). Purification and characterization of mouse fetal liver epithelial cells with high in vivo repopulation capacity. Hepatology *42*, 130–139.

Nierhoff, D., Levoci, L., Schulte, S., Goeser, T., Rogler, L.E., and Shafritz, D.A. (2007). New cell surface markers for murine fetal hepatic stem cells identified through high density complementary DNA microarrays. Hepatology *46*, 535–547.

Nitou, M., Sugiyama, Y., Ishikawa, K., and Shiojiri, N. (2002). Purification of fetal mouse hepatoblasts by magnetic beads coated with monoclonal anti-e-cadherin antibodies and their in vitro culture. Exp. Cell Res. *279*, 330–343.

Nowak, G., Ericzon, B.G., Nava, S., Jaksch, M., Westgren, M., and Sumitran-Holgersson, S. (2005). Identification of expandable human hepatic progenitors which differentiate into mature hepatic cells in vivo. Gut *54*, 972–979.

Nyamath, P., Alvi, A., Habeeb, A., Khosla, S., Khan, A.A., and Habibullah, C.M. (2007). Characterization of hepatic progenitors from human fetal liver using CD34 as a hepatic progenitor marker. World J. Gastroenterol. *13*, 2319–2323.

Okabe, M., Tsukahara, Y., Tanaka, M., Suzuki, K., Saito, S., Kamiya, Y., Tsujimura, T., Nakamura, K., and Miyajima, A. (2009). Potential hepatic stem cells reside in EpCAM+ cells of normal and injured mouse liver. Development *136*, 1951–1960.

Roelandt, P., Obeid, S., Paeshuyse, J., Vanhove, J., Van Lommel, A., Nahmias, Y., Nevens, F., Neyts, J., and Verfaillie, C.M. (2012). Human pluripotent stem cell-derived hepatocytes support complete replication of hepatitis C virus. J. Hepatol. *57*, 246–251.

Sackett, S.D., Li, Z., Hurtt, R., Gao, Y., Wells, R.G., Brondell, K., Kaestner, K.H., and Greenbaum, L.E. (2009). Foxl1 is a marker of bipotential hepatic progenitor cells in mice. Hepatology *49*, 920–929.

Schmelzer, E., Wauthier, E., and Reid, L.M. (2006). The phenotypes of pluripotent human hepatic progenitors. Stem Cells *24*, 1852–1858.

Schmelzer, E., Zhang, L., Bruce, A., Wauthier, E., Ludlow, J., Yao, H.L., Moss, N., Melhem, A., McClelland, R., Turner, W., et al. (2007). Human hepatic stem cells from fetal and postnatal donors. J. Exp. Med. *204*, 1973–1987.

Schwartz, R.E., Trehan, K., Andrus, L., Sheahan, T.P., Ploss, A., Duncan, S.A., Rice, C.M., and Bhatia, S.N. (2012). Modeling hepatitis C virus infection using human induced pluripotent stem cells. Proc. Natl. Acad. Sci. USA *109*, 2544–2548.

Sherwood, R.I., Jitianu, C., Cleaver, O., Shaywitz, D.A., Lamenzo, J.O., Chen, A.E., Golub, T.R., and Melton, D.A. (2007). Prospective isolation and global gene expression analysis of definitive and visceral endoderm. Dev. Biol. *304*, 541–555.

Shulla, A., and Randall, G. (2012). Hepatitis C virus-host interactions, replication, and viral assembly. Curr. Opin. Virol. *2*, 725–732.

Si-Tayeb, K., Lemaigre, F.P., and Duncan, S.A. (2010a). Organogenesis and development of the liver. Dev. Cell *18*, 175–189.

Si-Tayeb, K., Noto, F.K., Nagaoka, M., Li, J., Battle, M.A., Duris, C., North, P.E., Dalton, S., and Duncan, S.A. (2010b). Highly efficient generation of human hepatocyte-like cells from induced pluripotent stem cells. Hepatology *51*, 297–305.

Sondell, M., and Kanje, M. (2001). Postnatal expression of VEGF and its receptor flk-1 in peripheral ganglia. Neuroreport *12*, 105–108.

Srinivas, S., Watanabe, T., Lin, C.S., William, C.M., Tanabe, Y., Jessell, T.M., and Costantini, F. (2001). Cre reporter strains produced by targeted insertion of EYFP and ECFP into the ROSA26 locus. BMC Dev. Biol. *1*, 4.

Sullivan, G.J., Hay, D.C., Park, I.H., Fletcher, J., Hannoun, Z., Payne, C.M., Dalgetty, D., Black, J.R., Ross, J.A., Samuel, K., et al. (2010). Generation of functional human hepatic endoderm from human induced pluripotent stem cells. Hepatology *51*, 329–335.

Suzuki, A., Zheng, Y.W., Kaneko, S., Onodera, M., Fukao, K., Nakauchi, H., and Taniguchi, H. (2002). Clonal identification and characterization of self-renewing pluripotent stem cells in the developing liver. J. Cell Biol. *156*, 173–184.

Tada, S., Era, T., Furusawa, C., Sakurai, H., Nishikawa, S., Kinoshita, M., Nakao, K., Chiba, T., and Nishikawa, S. (2005). Characterization of mesendoderm: a diverging point of the definitive endoderm and mesoderm in embryonic stem cell differentiation culture. Development *132*, 4363–4374.

Takahashi, K., Tanabe, K., Ohnuki, M., Narita, M., Ichisaka, T., Tomoda, K., and Yamanaka, S. (2007). Induction of pluripotent stem cells from adult human fibroblasts by defined factors. Cell *131*, 861–872.

Tanaka, M., Okabe, M., Suzuki, K., Kamiya, Y., Tsukahara, Y., Saito, S., and Miyajima, A. (2009). Mouse hepatoblasts at distinct developmental stages are characterized by expression of EpCAM and DLK1: drastic change of EpCAM expression during liver development. Mech. Dev. *126*, 665–676.

Tanimizu, N., Nishikawa, M., Saito, H., Tsujimura, T., and Miyajima, A. (2003). Isolation of hepatoblasts based on the expression of Dlk/Pref-1. J. Cell Sci. *116*, 1775–1786.

Terrace, J.D., Currie, I.S., Hay, D.C., Masson, N.M., Anderson, R.A., Forbes, S.J., Parks, R.W., and Ross, J.A. (2007). Progenitor cell characterization and location in the developing human liver. Stem Cells Dev. *16*, 771–778.

Thomson, J.A., Itskovitz-Eldor, J., Shapiro, S.S., Waknitz, M.A., Swiergiel, J.J., Marshall, V.S., and Jones, J.M. (1998). Embryonic stem cell lines derived from human blastocysts. Science *282*, 1145–1147.

Touboul, T., Hannan, N.R., Corbineau, S., Martinez, A., Martinet, C., Branchereau, S., Mainot, S., Strick-Marchand, H., Pedersen, R., Di Santo, J., et al. (2010). Generation of functional hepatocytes from human embryonic stem cells under chemically defined conditions that recapitulate liver development. Hepatology *51*, 1754–1765.

White, A.C., Lavine, K.J., and Ornitz, D.M. (2007). FGF9 and SHH regulate mesenchymal Vegfa expression and development of the pulmonary capillary network. Development *134*, 3743–3752.

Wu, X., Robotham, J.M., Lee, E., Dalton, S., Kneteman, N.M., Gilbert, D.M., and Tang, H. (2012). Productive hepatitis C virus infection of stem cell-derived hepatocytes reveals a critical transition to viral permissiveness during differentiation. PLoS Pathog. *8*, e1002617.

Yoshida, T., Takayama, K., Kondoh, M., Sakurai, F., Tani, H., Sakamoto, N., Matsuura, Y., Mizuguchi, H., and Yagi, K. (2011). Use of human hepatocyte-like cells derived from induced pluripotent stem cells as a model for hepatocytes in hepatitis C virus infection. Biochem. Biophys. Res. Commun. *416*, 119–124.